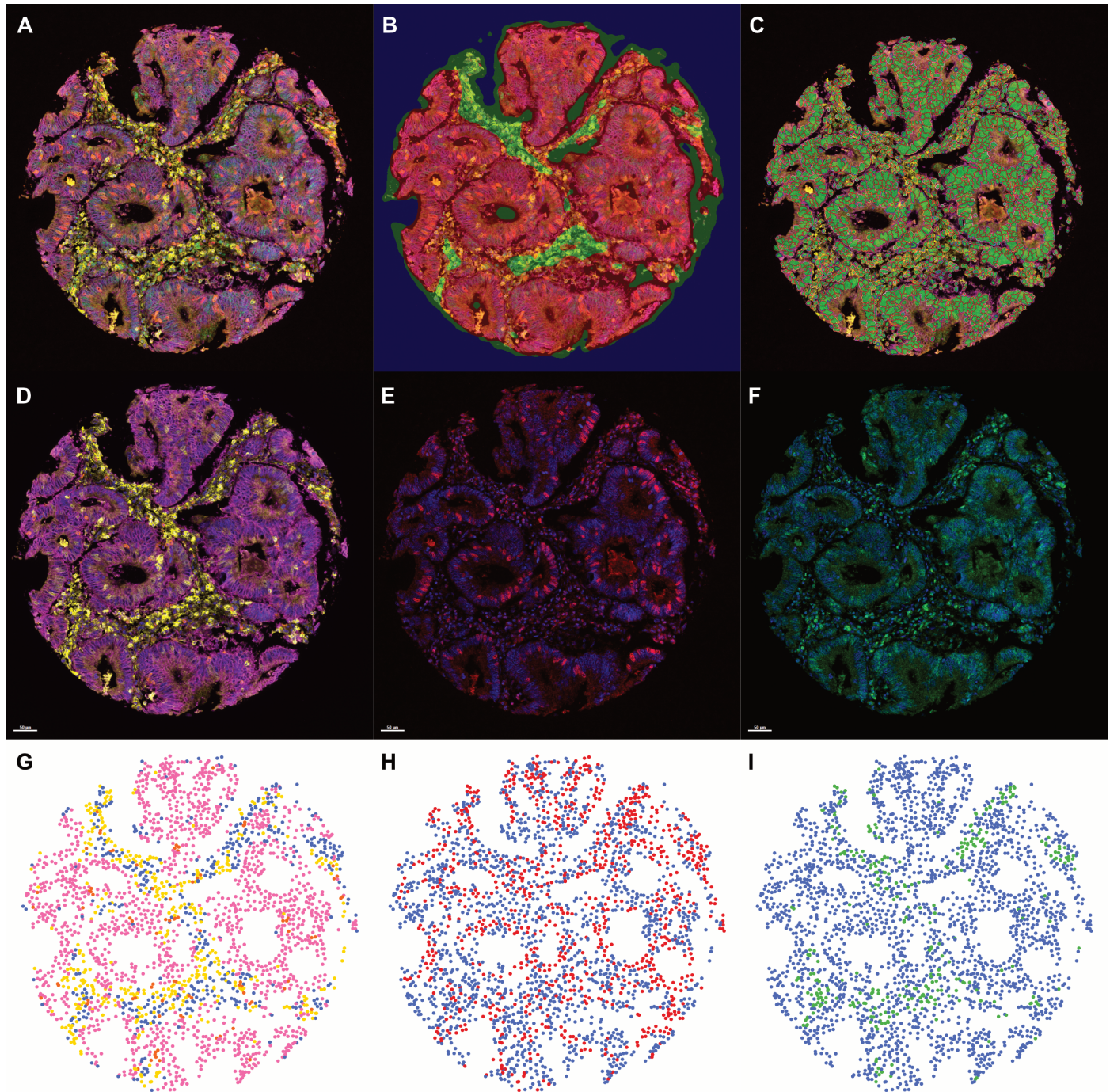


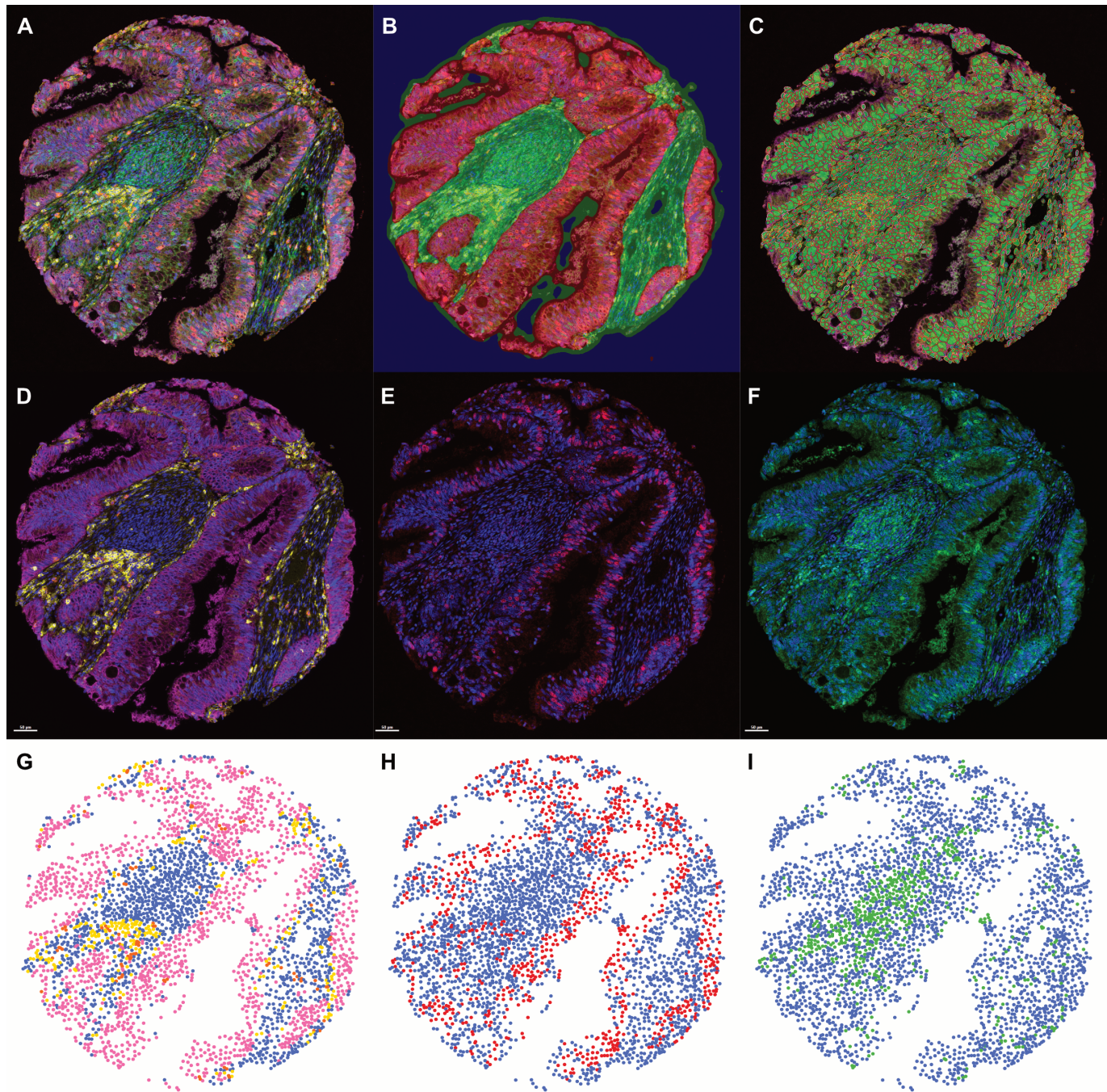
Supplementary Figure 1: Inform Training patient core 1- Tissue segmentation, cell segmentation and cell phenotyping

(A) Unmixed Image of one core fluorescence multiplex imaging of 6 markers CD4 (yellow); CD8 (orange); IL10 (green); Foxp3 (red); EpCAM (purple) nucleus (DAPI blue) **(B)** Tissue segmentation trained by EpCAM expression and selecting examples of each region: tumour epithelium (red), stroma (green) and blank (Blue). **(C)** Cell segmentation - Cells were identified and separated based on nuclear biomarkers (DAPI, Foxp3) and membrane biomarkers (CD4, CD8, EpCAM). For the phenotype identification, three separated schemes were used to assure accuracy. **(D, E, F)** show training images and **(G,H,I)** show the trained phenotypes with each dot representing a cell with blue dots representing other cells. **(D&G)** images depicting CD4+ (yellow), CD8+ (orange), EpCAM+ (Purple). **(E&H)** images depict Foxp3+ (red) **(F&I)** IL-10+ (green). All phenotypes were merged into the final phenotypes, which were used for all analyses.



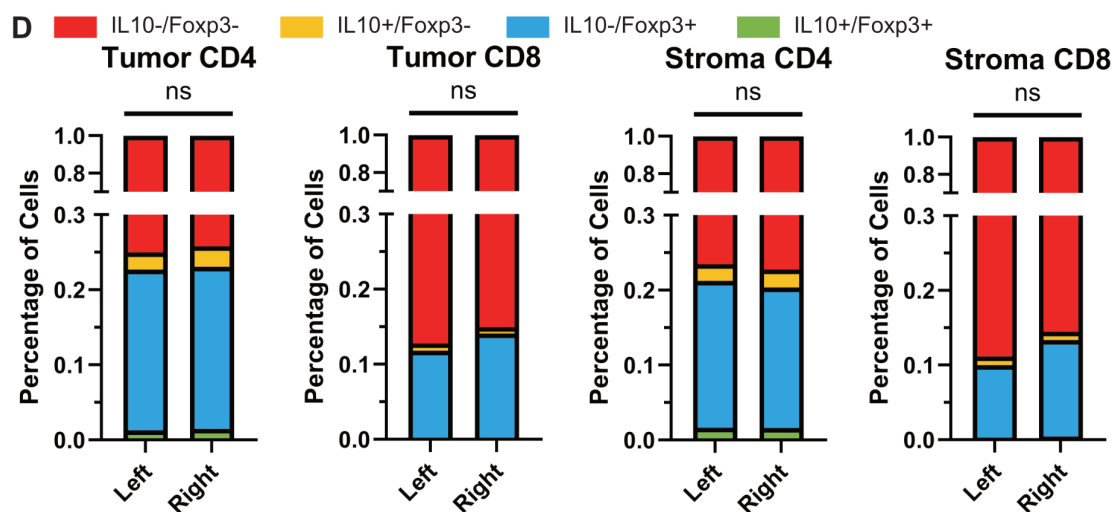
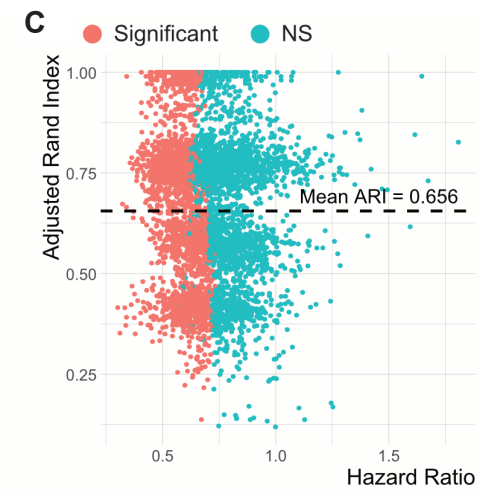
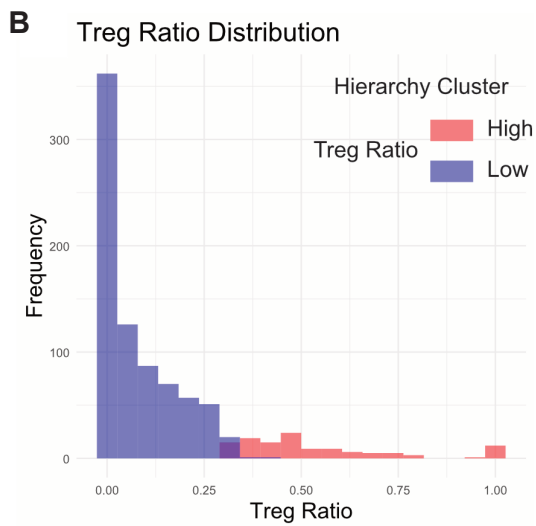
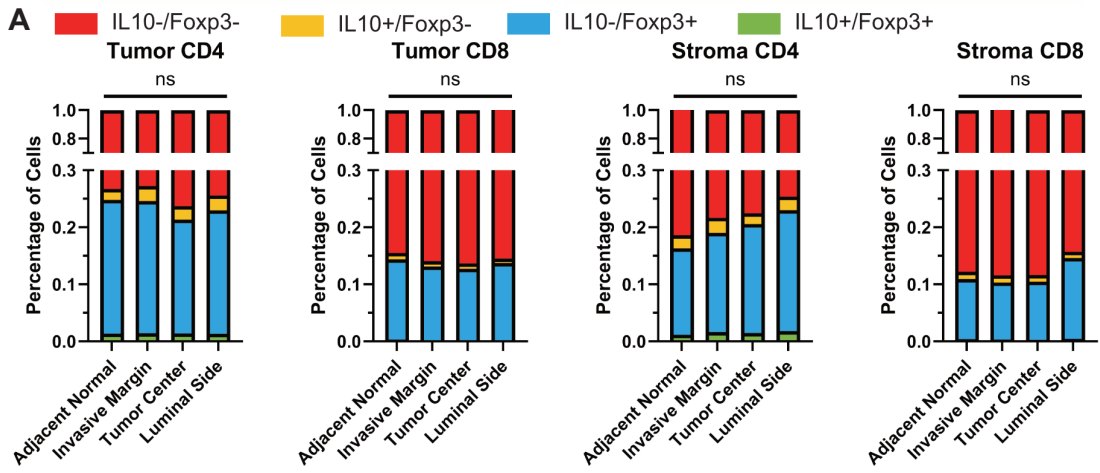
Supplementary Figure 2: Inform Training patient core 2- Tissue segmentation, cell segmentation and cell phenotyping

(A) Unmixed Image of one core fluorescence multiplex imaging of 6 markers CD4 (yellow); CD8 (orange); IL10 (green); Foxp3 (red); EpCAM (purple) nucleus (DAPI blue) **(B)** Tissue segmentation trained by EpCAM expression and selecting examples of each region: tumour epithelium (red), stroma (green) and blank (Blue). **(C)** Cell segmentation - Cells were identified and separated based on nuclear biomarkers (DAPI, Foxp3) and membrane biomarkers (CD4, CD8, EpCAM). For the phenotype identification, three separated schemes were used to assure accuracy. **(D, E, F)** show training images and **(G,H,I)** show the trained phenotypes with each dot representing a cell with blue dots representing other cells. **(D&G)** images depicting CD4+ (yellow), CD8+ (orange), EpCAM+ (Purple). **(E&H)** images depict Foxp3+ (red) **(F&I)** IL-10+ (green). All phenotypes were merged into the final phenotypes, which were used for all analyses.



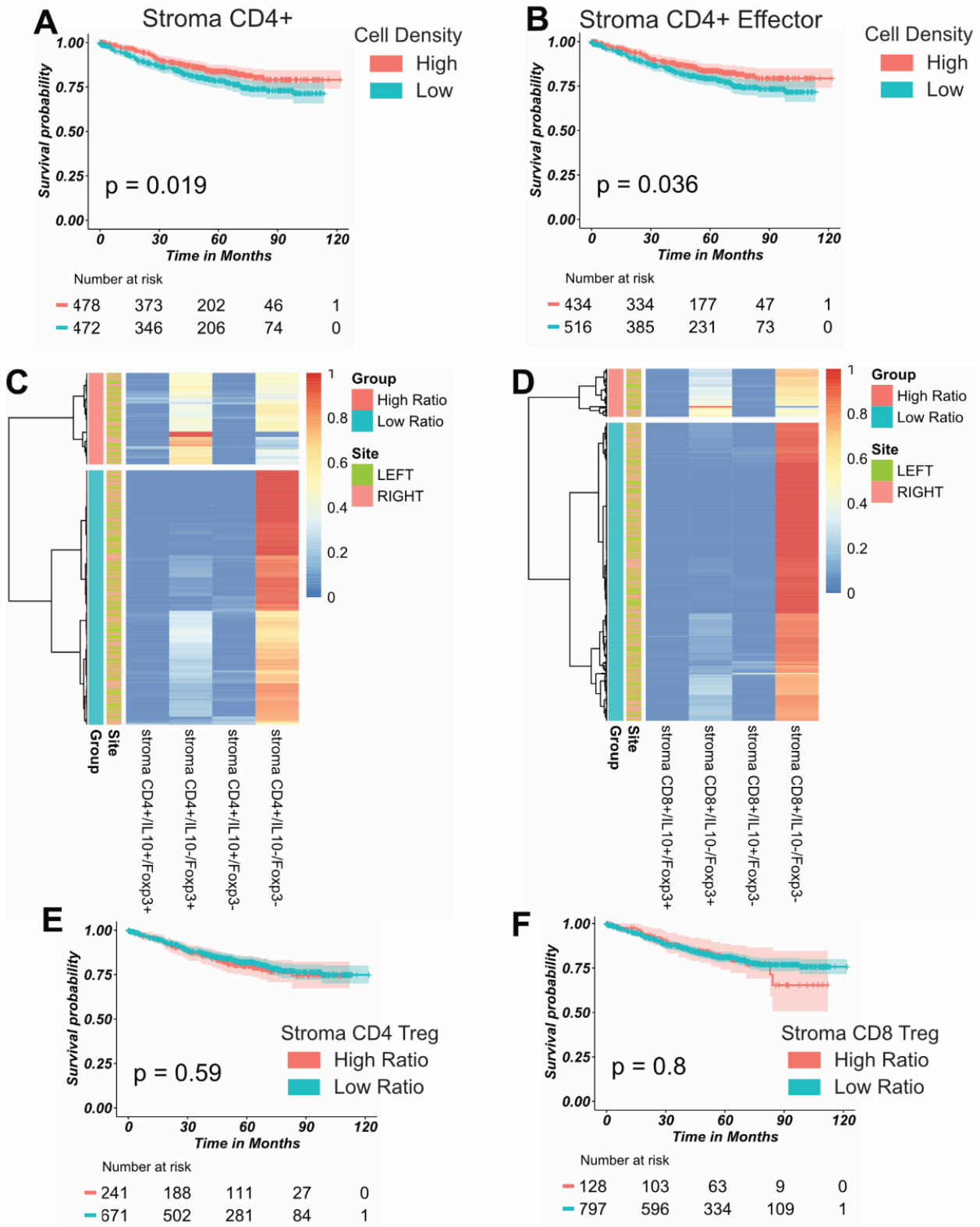
Supplementary Figure 3: Inform Training patient core 3- Tissue segmentation, cell segmentation and cell phenotyping

(A) Unmixed Image of one core fluorescence multiplex imaging of 6 markers CD4 (yellow); CD8 (orange); IL10 (green); Foxp3 (red); EpCAM (purple) nucleus (DAPI blue) **(B)** Tissue segmentation trained by EpCAM expression and selecting examples of each region: tumour epithelium (red), stroma (green) and blank (Blue). **(C)** Cell segmentation - Cells were identified and separated based on nuclear biomakers (DAPI, Foxp3) and membrane biomarkers (CD4, CD8, EpCAM). For the phenotype identification, three separated schemes were used to assure accuracy. **(D, E, F)** show training images and **(G,H,I)** show the trained phenotypes with each dot representing a cell with blue dots representing other cells. **(D&G)** images depicting CD4+ (yellow), CD8+ (orange), EpCAM+ (Purple). **(E&H)** images depict Foxp3+ (red) **(F&I)** IL-10+ (green). All phenotypes were merged into the final phenotypes, which were used for all analyses.



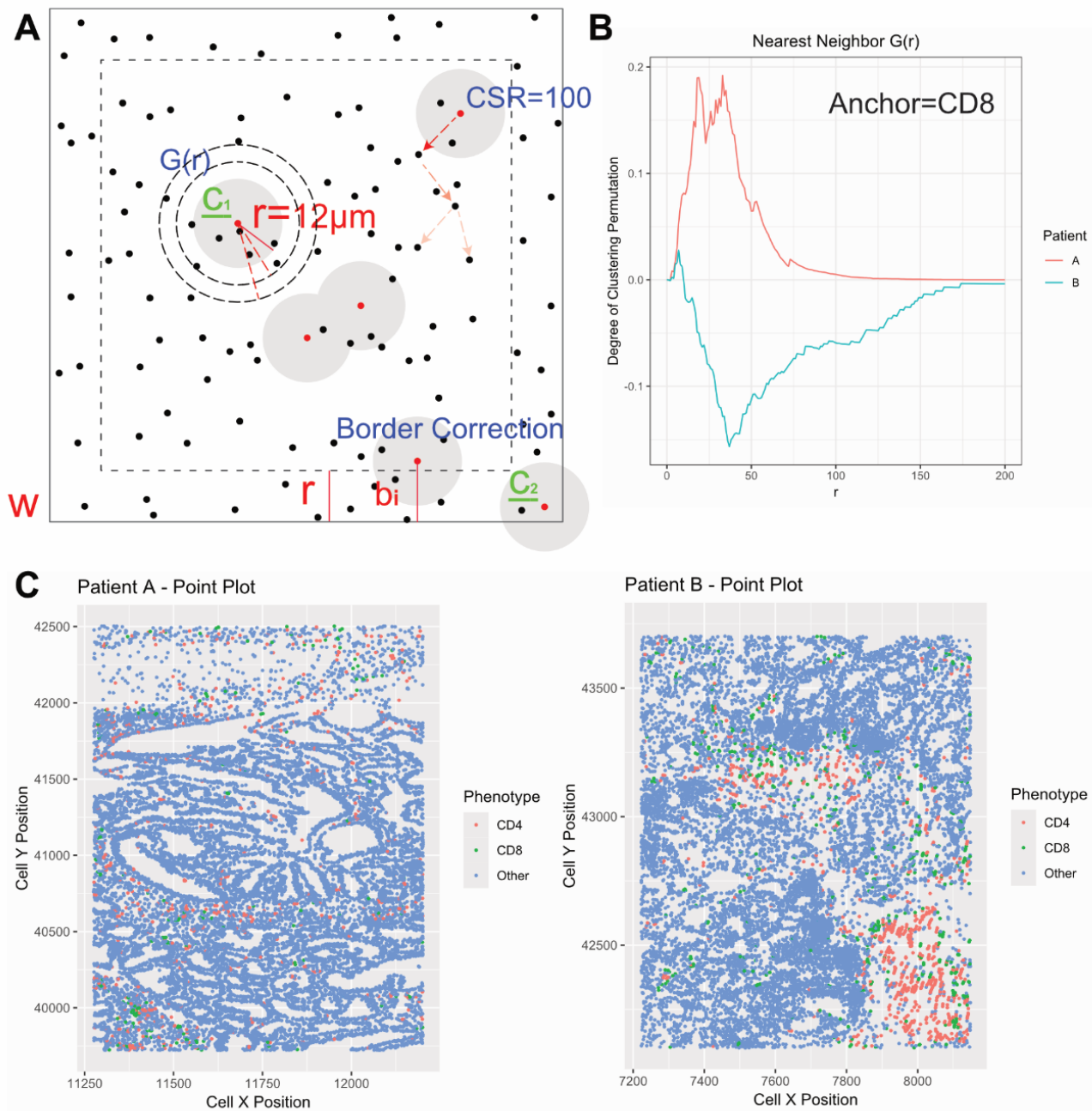
Supplementary Figure 4: Percentage of Treg cells in total CD4 and CD8 population.

(A) Bar graphs depicting comparison of the percentage of different Treg phenotypes of total CD4⁺ and CD8⁺ cells in the tumour epithelium and stroma areas of the adjacent normal, invasive margin, tumour centre and luminal side. IL10⁻Foxp3⁻ (Red), IL10⁺Foxp3⁻ (yellow), IL10⁻Foxp3⁺ (blue) and IL10⁺Foxp3⁺ (green). **(B)** Treg Ratio distribution **(C)** Bootstrapping was applied 5000 times (N= per analysis) (with replacement, no control on clinical characteristics). **(D)** Bar graphs depicting comparison of the percentage of different Treg phenotypes of total CD4⁺ and CD8⁺ cells in the tumour epithelium and stroma areas of the left and right-sided CRC. IL10⁻Foxp3⁻ (Red), IL10⁺Foxp3⁻ (yellow), IL10⁻Foxp3⁺ (blue) and IL10⁺Foxp3⁺ (green).



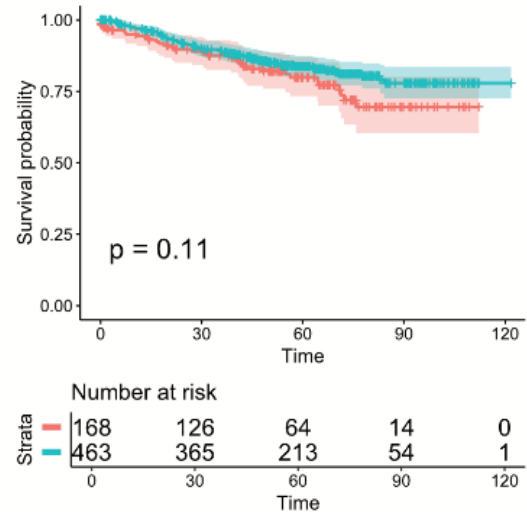
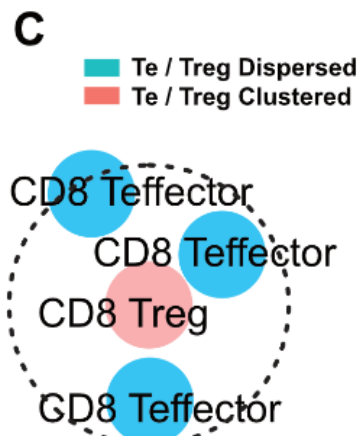
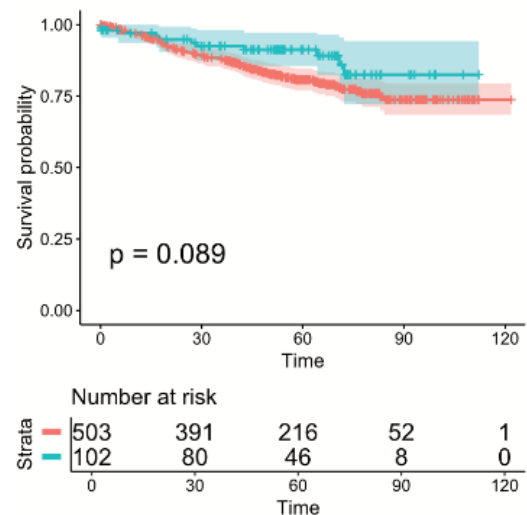
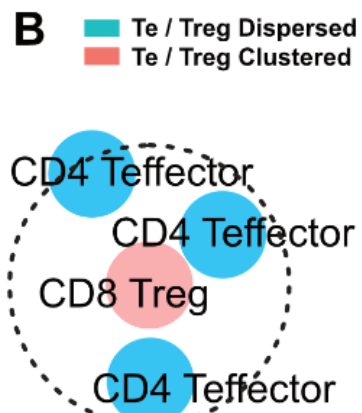
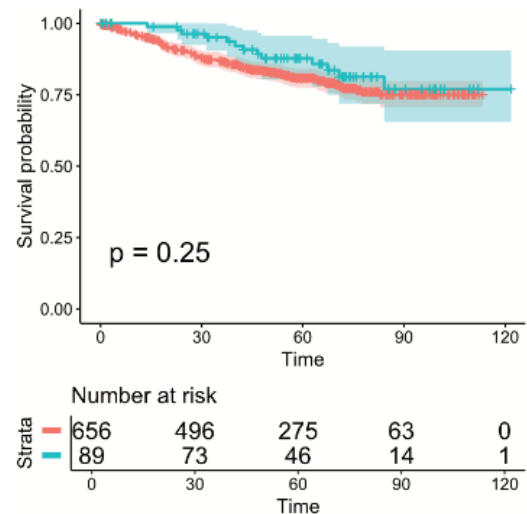
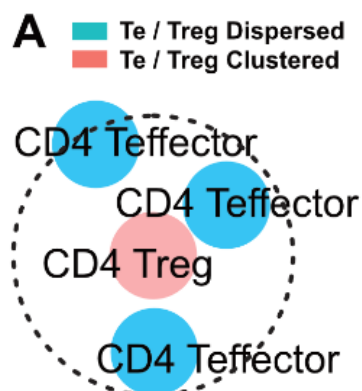
Supplementary Figure 5: Stromal CD4⁺ T effector cells associated with better survival but no effect of the ratio of stromal CD4 or CD8 Tregs on survival

Kaplan Meier survival curves for the density of **(A)** total CD4⁺ T cells and **(B)** Teff CD4⁺ T cells (CD4⁺Foxp3⁻IL10⁻) cells in the stroma **(C)** Patients tumours were divided into high and low ratios of CD4⁺ Treg to CD4 Teff cells in stroma by hierarchical clustering. **(D)** Patients were divided into high and low ratios of CD8 Treg cells to Teff cells the in stroma by hierarchical cluster. Kaplan-Meir survival curves for the density of **(E)** high and low ratios of stromal CD4⁺ Treg to CD4⁺ Teff cells and **(F)** high and low ratio of stromal CD8⁺ Treg to CD8⁺ Teff cells.



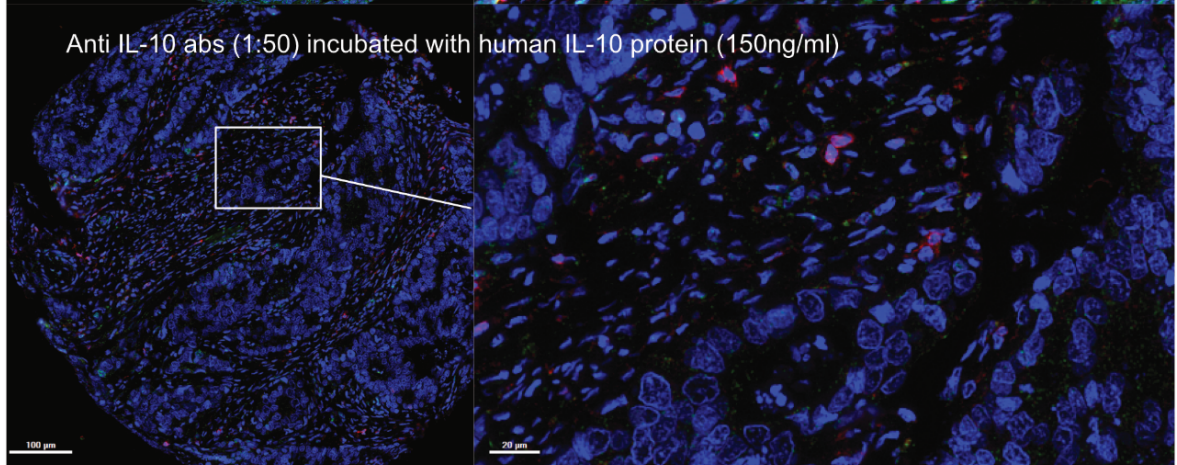
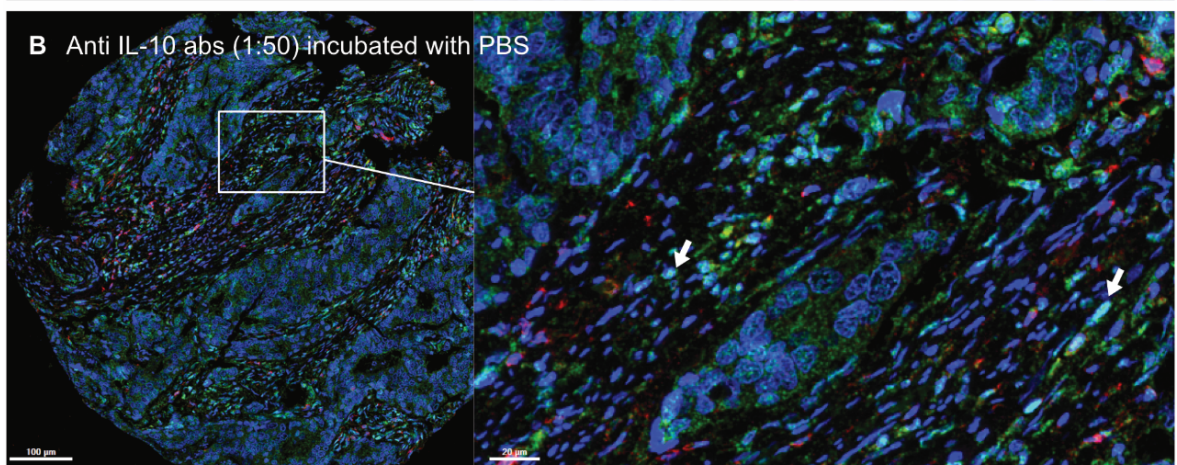
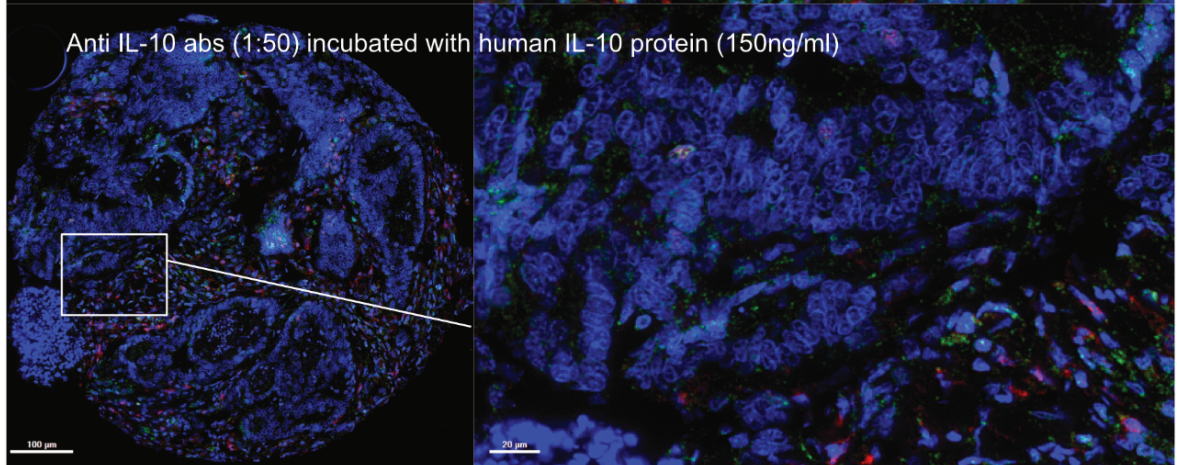
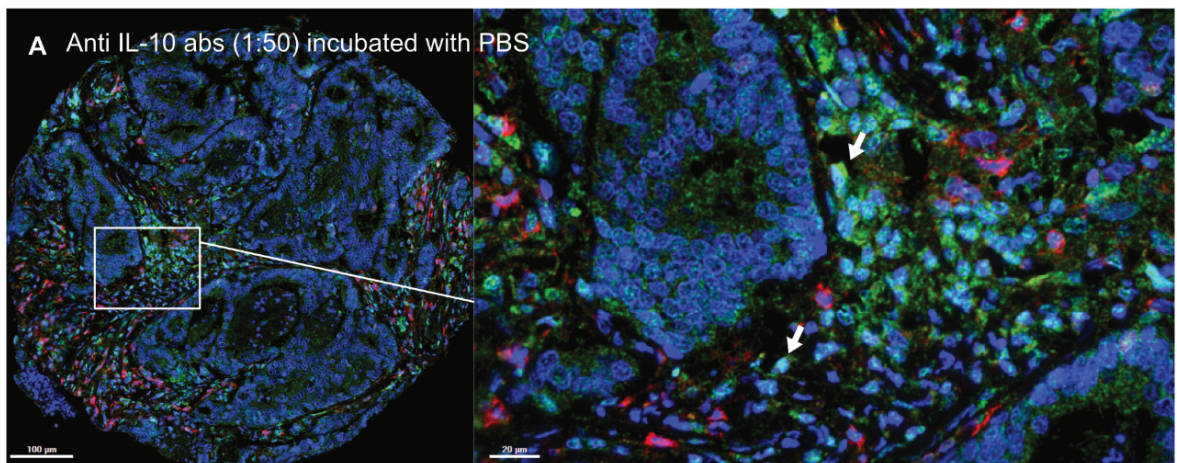
Supplementary Figure 6: No effect of cell-cell contact between CD4⁺ Teff-CD4⁺ Treg, CD4⁺ Teff-CD8⁺ Treg, or CD8⁺ Teff-CD8⁺ Treg and patients survival

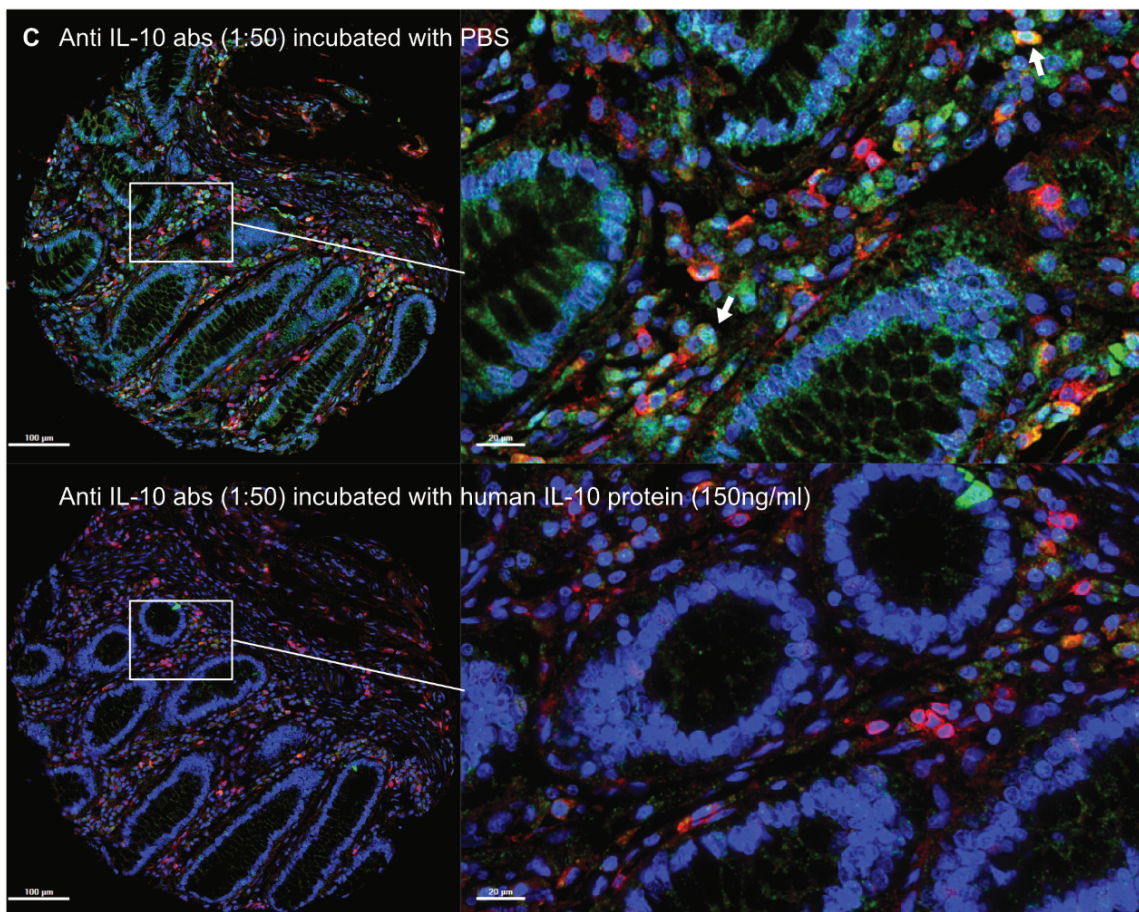
(A) G-cross function was calculated between CD4⁺ Teff cells and CD4⁺ Treg cells, and the prognostic value were tested by Kaplan-Meier survival analysis. **(B)** G-cross function was calculated between CD4⁺ Teff cells and CD8⁺ Treg cells, and the prognostic value was tested by Kaplan-Meier survival analysis. **(C)** G-cross function was calculated between CD8⁺ Teff to CD8⁺ Treg cells, and the prognostic value were tested by Kaplan-Meier survival analysis.



Supplementary Figure 7: No effect of cell-cell contact between CD4⁺ Teff-CD4⁺ Treg, CD4⁺ Teff-CD8⁺ Treg, or CD8⁺ Teff-CD8⁺ Treg and patients survival

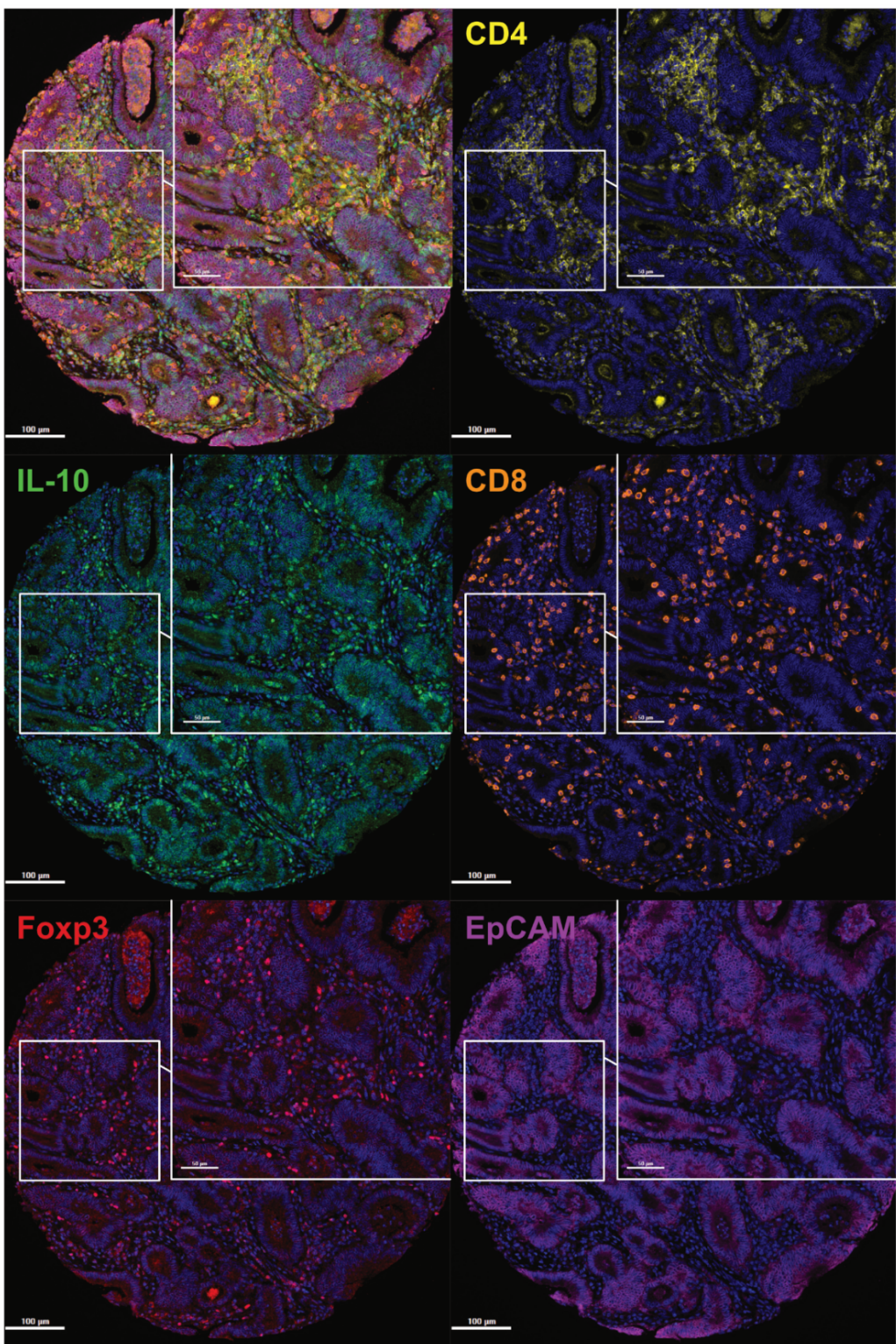
(A) G-cross function was calculated between CD4⁺ Teff cells and CD4⁺ Treg cells, and the prognostic value were tested by Kaplan-Meier survival analysis. **(B)** G-cross function was calculated between CD4⁺ Teff cells and CD8⁺ Treg cells, and the prognostic value was tested by Kaplan-Meier survival analysis. **(C)** G-cross function was calculated between CD8⁺ Teff to CD8⁺ Treg cells, and the prognostic value were tested by Kaplan-Meier survival analysis.





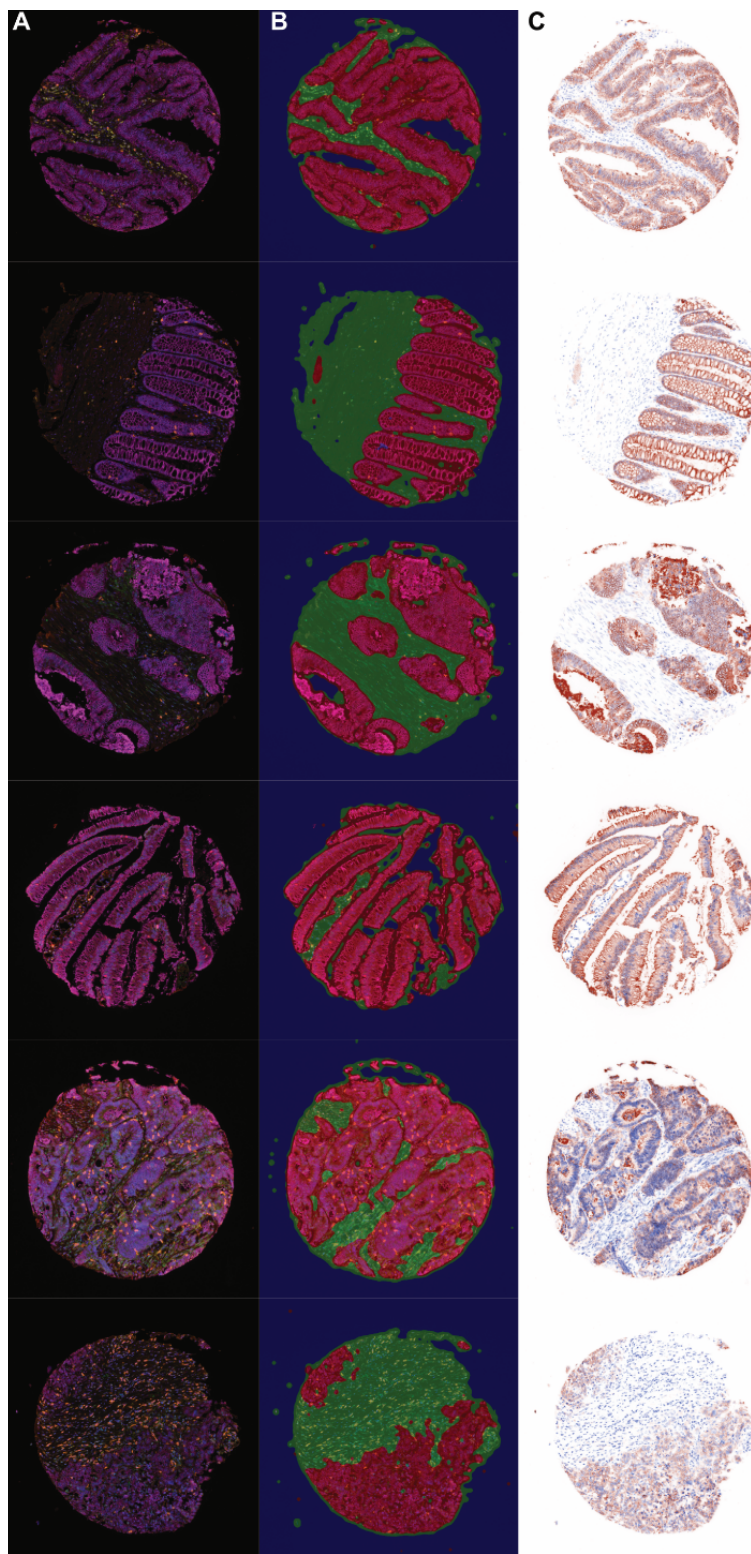
Supplementary Figure 8: Multiplex IHC immunoprobing with anti- IL10 antibody and with anti-IL-10 and IL10 protein block.

Anti- IL-10 antibody (1:50) was incubated with or without 150ng/ml human IL-10 protein at 4°C overnight (pH6). This was then used to immunoprobe control CRC slides. IL10+ cells are shown in green. CD4 was chosen as control. Anti-CD4 antibody immunoprobing is depicted in red. (A) (B) (C) represent three patients without human IL-10 protein (top panel) or with IL-10 protein block (bottom panel).



Supplementary Figure 9: Phenotype of Cells showing individual marker staining

Representative TMA core showing multiplex IHC with all markers (antibody-opal combinations). Individual images of the same core showing CD4⁺ cells (yellow), CD8⁺ cells (orange), IL10⁺ (green) Foxp3⁺ (Red) and EpCAM (magenta)



Supplementary Figure 10: Image Training by InForm® - examples of tissue segmentation

(A) The Acquired Image was unmixed **(B)** Tumour epithelium (red), Stroma (green) and Blank (blue) area was trained by manual annotations based on EpCAM expression depicting tumour epithelium. **(C)** Pseudo-pathological view based on EpCAM stain

Supplementary Table 1: Clinical Characteristics of CD8 Treg: CD8 effector T Ratio and CD4 T Effector Group in the tumour epithelium. Chi-squared-test analysis of clinical characteristic with CD8⁺Treg:CD8⁺ T cell ratio and with CD4⁺Teff density in the tumour epithelium.

Clinical Characteristic	CD8 Treg: CD8 effector T cells Ratio		P value	CD4 T Effector density Tumour epithelium		P value
	High n (%)	Low n (%)		High n (%)	Low n (%)	
Gender						
Female	50 (40.7)	339 (43.7)	0.520	209 (43.7)	198 (41.9)	0.580
Male	73 (59.3)	436 (56.3)		269 (56.3)	274 (58.1)	
Age						
≤69	77 (62.6)	377 (48.6)	0.004	234 (49)	250 (53)	0.216
>69	46 (37.4)	398 (51.4)		244 (51)	222 (47)	
Site						
Left	62 (50.4)	414 (53.4)	0.534	260 (54.4)	236 (50)	0.175
Right	61 (49.6)	361 (46.6)		218 (45.6)	236 (50)	
TNM stage						
I	15 (12.2)	133 (17.2)	0.050	83 (17.4)	69 (14.6)	0.125
II	42 (34.1)	324 (41.8)		204 (42.7)	181 (38.3)	
III	47 (38.2)	274 (25.4)		145 (30.3)	160 (33.9)	
IV	19 (15.4)	77 (9.9)		46 (9.6)	62 (13.1)	
MSS/MSI						
MSS	101 (85.6)	631 (82.8)	0.452	395 (83.9)	377 (82.5)	0.577
MSI	17 (14.4)	131 (17.2)		76 (16.1)	80 (17.5)	